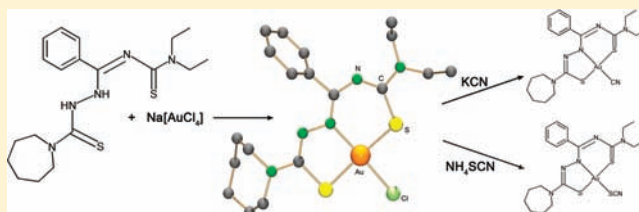


Neutral Gold Complexes with Tridentate SNS Thiosemicarbazide Ligands^{||}Pedro I. da S. Maia,[†] Hung Huy Nguyen,[‡] Daniela Ponader,[§] Adelheid Hagenbach,[§] Silke Bergemann,[⊥] Ronald Gust,[⊥] Victor M. Deflon,[†] and Ulrich Abram^{*§}[†]Instituto de Química de São Carlos, Universidade de São Paulo, CP 780, São Carlos-São Paulo, Brazil[‡]Department of Chemistry, Hanoi University of Science, 19 Le Thanh Tong, Hanoi, Vietnam[§]Institute of Chemistry and Biochemistry, Freie Universität Berlin, Fabeckstr. 34-36, D-14195 Berlin, Germany[⊥]Institute of Pharmacy, Freie Universität Berlin, Königin-Louise-Str. 2 and 4, D-14195 Berlin, Germany

S Supporting Information

ABSTRACT: Na[AuCl₄]·2H₂O reacts with tridentate thiosemicarbazide ligands, H₂L1, derived from *N*-[*N'*,*N'*-dialkylamino(thiocarbonyl)]benzimidoyl chloride and thiosemicarbazides under formation of air-stable, green [AuCl(L1)] complexes. The organic ligands coordinate in a planar SNS coordination mode. Small amounts of gold(I) complexes of the composition [AuCl(L3)] are formed as side-products, where L3 is an S-bonded 5-diethylamino-3-phenyl-1-thiocarbamoyl-1,2,4-triazole. The formation of the triazole L3 can be explained by the oxidation of H₂L1 to an intermediate thiatriazine L2 by Au³⁺, followed by a desulfurization reaction with ring contraction. The chloro ligands in the [AuCl(L1)] complexes can readily be replaced by other monoanionic ligands such as SCN⁻ or CN⁻ giving [Au(SCN)(L1)] or [Au(CN)(L1)] complexes. The complexes described in this paper represent the first examples of fully characterized neutral Gold(III) thiosemicarbazone complexes. All the [AuCl(L1)] compounds present a remarkable cell growth inhibition against human MCF-7 breast cancer cells. However, systematic variation of the alkyl groups in the *N*(4)-position of the thiosemicarbazone building blocks as well as the replacement of the chloride by thiocyanate ligands do not considerably influence the biological activity. On the other hand, the reduction of Au^{III} to Au^I leads to a considerable decrease of the cytotoxicity.



■ INTRODUCTION

Thiosemicarbazones are versatile ligands of considerable significance with respect to their variable coordination behavior and promising biological and pharmaceutical properties,^{1,2} and gold complexes are classical inorganic pharmaceuticals for treatment of arthritis and rheumatism.³ Gold complexes with thiosemicarbazones are comparatively rare, and some of the recently published papers deal with gold(I) compounds.⁴ Of particular interest, however, should be gold(III) compounds which are isoelectronic with Pt(II) and also prefer square-planar complexes. However, the first gold(III) compound with a thiosemicarbazone ligand was published only in 1998,⁵ and afterward only few complexes of this type have been reported. In most of the published papers, the Au(III) thiosemicarbazone complexes without an organometallic framework, which is provided by the precursor dichloro[2-(dimethylaminomethyl)-phenyl-*C*¹,*N*]-gold(III), [Au(damp-*C*¹,*N*)Cl₂], are reported to be not stable, which leads to reduction to Au(I) or to the formation of decomposition products.⁶ Indeed, only a few gold(III) thiosemicarbazone complexes without the damp ligand have been structurally characterized up to now,^{7–9} and no neutral complex have been reported. A very recent work evaluates first the potential of radioactive ¹⁹⁸Au thiosemicarbazone complexes for nuclear therapeutic applications.⁹

A new class of tridentate thiocarbamoylbenzamidines containing an additional thiosemicarbazone moiety and their rhenium complexes have been reported recently together with the biological activity of the organic compounds and some of their oxorhenium(V) and nitridorhenium(V) complexes.¹⁰ The novel chelators, which combine a thiosemicarbazide moiety with a thiourea building block can readily be prepared from the corresponding benzimide chloride and various thiosemicarbazides (Chart 1).¹⁰

Here, we report about the synthesis and characterization of a series of new gold(III) complexes with the potentially tridentate ligands H₂L1, as well as a first evaluation of their in vitro cytotoxic activity as the basis for their evaluation as potential anticancer and antituberculosis drugs.

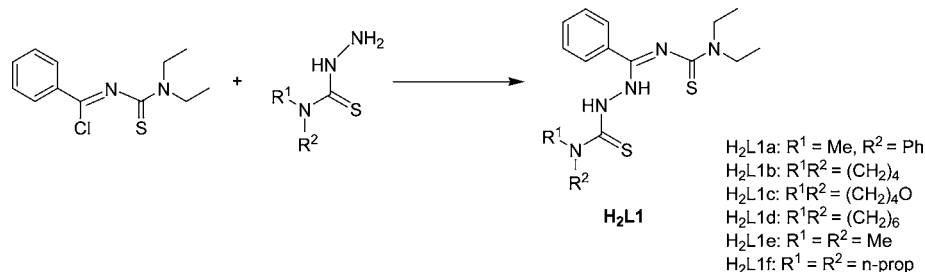
■ EXPERIMENTAL SECTION

Materials. All reagents used in this study were reagent grade and used without further purification. The solvents were dried and used freshly distilled prior to use unless otherwise stated. Na[AuCl₄]·2H₂O was prepared by a standard procedure.¹¹ The synthesis of *N*-[(diethylamino)(thiocarbonyl)]benzimidoyl chloride was performed by the procedure of Beyer and Widera.¹² The thiosemicarbazides were

Received: August 31, 2011

Published: January 10, 2012

Chart 1. Synthesis of the Ligands Used Throughout This Study



prepared by methods reported before.¹³ The compounds H₂L1a, H₂L1b, H₂L1d, and H₂L1e were prepared as reported in our previous papers.^{10,14}

Physical Measurements. IR spectra were measured as CsI pellets on a Shimadzu IR Prestige-21 spectrophotometer between 250 and 4000 cm⁻¹. ¹H and ¹³C NMR spectra were taken with a JEOL 400 MHz multinuclear spectrometer. ESI⁺ mass spectra were measured with an Agilent 6210 ESI-TOF (Agilent Technologies). The elemental analyses of carbon, hydrogen, nitrogen, and sulfur were determined using a Heraeus vario EL elemental analyzer. The elemental analyses of the gold compounds showed systematically too low values for hydrogen and sometimes carbon (in some cases in a significant extent). This might be caused by an incomplete combustion of the metal compounds and/or hydride formation, and does not refer to impure samples. Similar findings have been observed for analogous rhenium complexes with the same type of ligands before.¹⁰ We left these values uncorrected. Additional proof for the identity of the products is given by high-resolution mass spectra for selected representatives. The conductivities of some representative complexes were measured in dimethylsulfoxide (DMSO) with an Orion Star Series conductometer.

Preparations of the Ligands. To a mixture containing the desired thiosemicarbazide (2 mmol) and 12 mmol of Et₃N in dry tetrahydrofuran (THF, 10 mL), *N*-(*N,N'*-diethylaminothiocarbonyl)-benzimidoyl chloride (2 mmol) was added. The mixture was stirred for 4 h at room temperature. The colorless precipitate of NEt₃·HCl was filtered off, and the solvent of the filtrate was removed under reduced pressure. The residue was dissolved in diethyl ether (10 mL) and stored at -20 °C. The colorless solid of H₂L1, which deposited from this solution, was filtered off, washed with *n*-hexane, and dried under vacuum.

The compounds obtained by this procedure were used for the syntheses of the complexes without further purification.

H₂L1c. Colorless needles. Yield: 71% (540 mg). Anal. Calcd for C₁₇H₂₃N₅O₂: C, 53.80; H, 6.64; N, 18.45; S, 16.89%. Found: C, 53.81; H, 6.46; N, 18.20; S, 16.59%. IR (ν_{max}/cm⁻¹): 3182 s (NH), 1636 vs (C=N). ¹H NMR (CDCl₃, ppm): 1.04 (t, *J* = 7.1 Hz, 3H, CH₃), 1.21 (t, *J* = 7.0 Hz, 3H, CH₃), 3.51 (q, *J* = 7.1 Hz, 2H, CH₂), 3.68 (t, *J* = 4.8 Hz, 4H, N-CH₂ morph), 3.82–3.89 (m, 6H, CH₂ + O-CH₂ morph), 7.42–7.49 (m, 3H, Ph), 7.86 (d, *J* = 7.8 Hz, 2H, *o*-Ph), 9.49 (s, 1H, NH), 10.11 (s, 1H, NH). ¹³C NMR (CDCl₃, δ, ppm): 12.4, 13.0 (CH₃), 45.0, 46.4 (NCH₂, ethyl), 48.5 (NCH₂, morpholine), 66.1 (OCH₂), 127.7, 128.8, 131.6, 132.8 (Ph), 148.9 (C=N), 179.7, 183.2 (C=S). ESI⁺ MS (*m/z*, assignment): 402 (M + Na)⁺, 418 (M + K)⁺.

H₂L1f. Colorless powder. Yield: 75% (590 mg). Anal. Calcd for C₁₉H₃₁N₅S₂: C, 57.98; H, 7.94; N, 17.79; S, 16.29%. Found: C, 58.05; H, 7.91; N, 17.47; S, 16.43%. IR (ν_{max}/cm⁻¹): 3240 s (NH), 1632 vs (C=N). ¹H NMR (CDCl₃, ppm): 0.91 (t, *J* = 7.5 Hz, 6H, -CH₂CH₂CH₃), 0.99 (t, *J* = 7.1 Hz, 3H, -CH₂CH₃), 1.23 (t, *J* = 7.1 Hz, 3H, -CH₂CH₃), 1.62 (sex, *J* = 7.5, 4H, -CH₂CH₂CH₃), 3.53 (m, 6H, -CH₂CH₂CH₃ + -CH₂CH₃), 3.90 (q, *J* = 7.1 Hz, 2H, -CH₂CH₃), 7.37–7.47 (m, 3H, Ph), 7.89 (d, *J* = 6.8 Hz, 2H, *o*-Ph), 9.67 (s, 1H, NH), 9.87 (s, 1H, NH). ¹³C NMR (CDCl₃, δ, ppm): 11.3, 12.4, 12.9 (CH₃), 20.4 (CH₂, *n*-propyl), 44.6, 46.2 (NCH₂), 127.7, 128.7, 131.4, 133.1 (Ph), 149.2 (C=N), 178.5, 183.2 (C=S). ESI⁺ MS (*m/z*, assignment): 416 [M + Na]⁺, 432 [M + K]⁺.

Synthesis of the [Au^{III}Cl(L1)] Type Complexes. 0.1 mmol of H₂L1 was added to a solution of 0.1 mmol of Na[AuCl₄]·2H₂O in MeOH (1 mL). The resulting solutions were stirred for 2 h at room temperature. Green solids precipitated during this time. The precipitates were filtered off, washed with cold MeOH, *n*-hexane, and dried in air. Recrystallization from MeOH/CH₂Cl₂ mixtures gave green crystals. By slow evaporation of the remaining mother solutions, small amounts (approximately 1–20%) of colorless solids appeared, which could only be separated in reasonable amounts for the H₂L1d derivative. It could be characterized as a gold(I) complex of a cyclization product of the ligand, [AuCl(L3d)].

[Au^{III}Cl(L1a)] (1). Yield: 51% (32 mg). Anal. Calcd for C₂₀H₂₃AuClN₅S₂: C, 38.13; H, 3.69; N, 11.12; S, 10.18%. Found: C, 37.92; H, 3.23; N, 11.21; S, 10.02%. IR (ν_{max}/cm⁻¹): 1552 m (C=N), 1489 vs (C=C), 335 w (Au-Cl). ¹H NMR (CDCl₃, ppm): 1.16 (t, *J* = 7.2 Hz, 3H, CH₃), 1.24 (t, *J* = 7.2 Hz, 3H, CH₃), 3.12 (s, 3H, N-CH₃), 3.66 (q, *J* = 7.2 Hz, 4H, methylene), 7.15–7.32 (m, 8H, Ph), 7.58–7.61 (m, 2H, *o*-Ph). ¹³C NMR (CDCl₃, δ, ppm): 12.7, 13.0 (CH₃), 43.5 (NCH₃), 45.3, 47.5 (NCH₂), 126.8, 127.0, 127.3, 129.1, 129.4, 137.9, 146.1 (Ph), 155.3, 158.3, 160.2 (C=N). ESI⁺ MS (*m/z*, assignment): 594 [M-Cl]⁺, 630 [M]⁺, 652 [M + Na]⁺, 668 [M+K]⁺, 991 [Au(L1a)(L2a)]⁺. High resolution MS of molecular ion [M+H]⁺ Calcd: 630.0827, Found: 630.0824.

[Au^{III}Cl(L1b)] (2). Yield: 47% (28 mg). Anal. Calcd for C₁₇H₂₃AuClN₅S₂: C, 34.38; H, 3.90; N, 11.79; S, 10.80%. Found: C, 33.98; H, 3.52; N, 11.75; S, 11.02%. IR (ν_{max}/cm⁻¹): 1560 m (C=N), 1500 vs (C=C), 341 w (Au-Cl). ¹H NMR (CDCl₃, ppm): 1.12–1.18 (m, 6H, CH₃), 1.80 (s, br, 4H, CH₂), 3.15 (s, br, 4H, CH₂), 3.63 (s, br, 4H, NCH₂, pyrrolidine), 7.27–7.36 (m, 3H, Ph), 7.58 (dd, ³*J* = 6.7 Hz, ⁴*J* = 2.3 Hz, 2H, *o*-Ph). ESI⁺ MS (*m/z*, assignment): 558 [M-Cl]⁺, 594 [M+H]⁺, 616 [M + Na]⁺, 632 [M+K]⁺, 919 [Au(L1b)(L2b)]⁺. High resolution MS of molecular ion [M+H]⁺ Calcd: 594.0827, Found: 594.0811.

[Au^{III}Cl(L1c)] (3). Yield: 48% (29 mg). Anal. Calcd for C₁₇H₂₃AuClN₅O₂: C, 33.48; H, 3.80; N, 11.48; S, 10.51%. Found: C, 33.14; H, 3.38; N, 11.51; S, 10.38%. IR (ν_{max}/cm⁻¹): 1556 m (C=N), 1500 vs (C=C), 339 w (Au-Cl). ¹H NMR (CDCl₃, ppm): 1.14–1.28 (m, 6H, CH₃), 3.17 (t, *J* = 4.8 Hz, 4H, N-CH₂), 3.55 (t, *J* = 4.8 Hz, 4H, O-CH₂), 3.68 (q, *J* = 7.0 Hz, 4H, methylene), 7.28–7.30 (m, 3H, Ph), 7.51 (d, *J* = 7.8 Hz, 2H, *o*-Ph). ¹³C NMR (CDCl₃, δ, ppm): 12.7, 13.0 (CH₃), 45.3, 47.5 (NCH₂, ethyl), 49.7 (NCH₂, morpholine), 66.5 (OCH₂), 127.3, 129.3, 129.4, 137.7 (Ph), 155.1 (C=N), 158.0 (C=N), 160.9 (C=N). ESI⁺ MS (*m/z*, assignment): 574 [M-Cl]⁺, 610 [M+H]⁺, 632 [M + Na]⁺, 648 [M+K]⁺, 951 [Au(L1c)(L2c)]⁺, 1241 [2M+Na]⁺. Molar conductivity (10⁻³ M, DMSO): 2.5 S cm² mol⁻¹. High resolution MS of molecular ion [M+H]⁺ Calcd: 610.0776, Found: 610.0784.

[Au^{III}Cl(L1d)] (4). Yield: 56% (35 mg). Anal. Calcd for C₁₉H₂₇AuClN₅S₂: C, 36.69; H, 4.38; N, 11.26; S, 10.31%. Found: C, 36.43; H, 3.68; N, 11.31; S, 10.71%. IR (ν_{max}/cm⁻¹): 1549 m (C=N), 1497 vs (C=C), 337 w (Au-Cl). ¹H NMR (CDCl₃, ppm): 1.14 (t, *J* = 7.0 Hz, 3H, CH₃), 1.21 (t, *J* = 8.8 Hz, 3H, CH₃), 1.43 (s, br, 4H, CH₂, azepine), 1.50 (s, br, 4H, CH₂, azepine), 3.28 (t, *J* = 5.8 Hz, 4H, NCH₂ azepine), 3.63 (m, 4H, NCH₂CH₃), 7.27–7.25 (m, 3H, Ph), 7.51 (dd, *J* = 6.6 Hz, *J* = 2.5 Hz, 2H, *o*-Ph). ¹³C NMR (CDCl₃, δ, ppm): 12.9, 13.0 (CH₃), 26.9, 28.4 (CH₂, azepine), 45.1, 47.3 (NCH₂, ethyl), 52.7 (NCH₂, azepine), 127.2, 128.8, 129.3, and 138.2 (Ph),

Table 1. X-ray Structure Data Collection and Refinement Parameters for [Au^{III}Cl(L1d)] (4), [Au^{III}Cl(L1e)] (5), [Au^ICl(L3d)] (4a), [Au^{III}(SCN)(L1c)] (8), [Au(CN)(L1c)] (9), and [Au(CN)(L1d)] (10)

	4	5	4a	8	9	10
formula	C ₁₉ H ₂₇ AuClN ₅ S ₂	C ₁₅ H ₂₁ AuClN ₅ S ₂	C ₁₉ H ₂₇ AuClN ₅ S	C ₁₈ H ₂₃ AuN ₆ OS ₃	C ₁₈ H ₂₃ AuN ₆ OS ₂	C ₂₀ H ₂₇ AuN ₆ S ₂
Fw	621.99	567.90	589.93	632.57	600.51	612.56
crystal system	orthorhombic	monoclinic	monoclinic	monoclinic	monoclinic	orthorhombic
space group	<i>Pbca</i>	<i>P2₁/n</i>	<i>P2₁/n</i>	<i>P2₁/c</i>	<i>P2₁/c</i>	<i>Pbca</i>
<i>a</i> (Å)	13.7878(6)	10.8864(7)	8.0871(7)	11.833(1)	11.884(1)	13.927(1)
<i>b</i> (Å)	9.7254(5)	8.0631(6)	23.774(2)	8.2302(6)	14.571(1)	9.6701(8)
<i>c</i> (Å)	33.280(2)	22.032(1)	11.614(1)	22.484(2)	13.368(1)	33.253(3)
α (deg)	90	90	90	90	90	90
β (deg)	90	99.57(1)	106.44(1)	95.41(1)	114.85(1)	90
γ (deg)	90	90	90	90	90	90
<i>V</i> (Å ³)	4462.6(4)	1907.0(2)	2141.7(3)	2179.9(3)	2100.4(3)	4478.4(7)
<i>Z</i>	8	4	4	4	4	8
ρ_{calcd} (g·cm ⁻³)	1.852	1.978	1.830	1.927	1.899	1.817
μ (mm ⁻¹)	6.915	8.081	7.105	7.059	7.224	6.775
reflections collected	45569	13168	16009	13047	13384	13768
reflections unique/ <i>R</i> _{int}	6026/0.0957	5115/0.0590	5757/0.0588	5836/0.0739	5609/0.0794	5927/0.0605
data/restraints/param.	6026/0/256	5115/0/222	5757/0/247	5836/0/265	5609/0/256	5927/0/265
absorption correction	integration	integration	integration	integration	integration	integration
max/min transmission	0.5417/0.3142	0.7692/0.3744	0.4632/0.2311	0.7088/0.2120	0.6790/0.3397	0.4418/0.1816
<i>R</i> ₁ [<i>I</i> > 2 σ (<i>I</i>)]	0.0500	0.0465	0.0345	0.0559	0.0394	0.0631
w <i>R</i> ₂ [<i>I</i> > 2 σ (<i>I</i>)]	0.1199	0.1046	0.0776	0.1336	0.0813	0.1628
GOF	0.883	1.002	1.089	0.984	0.868	1.027

153.6, 157.3, 159.9 (C=N). ESI⁺ MS (*m/z*, assignment): 586 [M-Cl]⁺, 622 [M+H]⁺, 644 [M + Na]⁺, 660 [M+K]⁺, 975 [Au(L1d)-(L2d)]⁺. Molar conductivity (10⁻³ M, DMSO): 2.2 S cm² mol⁻¹. High resolution MS of molecular ion [M+H]⁺ Calcd: 622.1140, Found: 622.1129.

[Au^ICl(L3d)] (4a). Yield: 17% (10 mg). Anal. Calcd for C₁₉H₂₇AuClN₅S: C, 38.68; H, 4.61; N, 11.87; S, 5.44%. Found: C, 38.65; H, 4.21; N, 11.76; S, 5.37%. IR (ν_{max} /cm⁻¹): 1585 vs (C=N), 1508 vs (C=C), 332 w (Au-Cl). ¹H NMR (CDCl₃, ppm): 1.32 (t, *J* = 7.1 Hz, 6H, CH₃), 1.4–2.2 (m, br, 8H, CH₂, azepine), 3.4–3.6 (m, br, 4H, NCH₂, azepine), 3.9–4.1 (m, br, 4H, NCH₂CH₃), 7.37–7.39 (m, 3H, Ph), 8.01 (dd, *J* = 4.5 Hz, *J* = 2.1 Hz, 2H, *o*-Ph). ¹³C NMR (CDCl₃, δ , ppm): 12.8 (CH₃), 25.7, 26.0, 27.6, 27.8 (CH₂, azepine), 44.7 (N-CH₂), 55.3, 56.3 (N-CH₂, azepine), 127.0, 128.4, 129.9, 130.0 (Ph), 159.6, 162.7 (C=N), 180.6 (C=S). ESI⁺ MS (*m/z*, assignment): 358 [L3d + H]⁺, 380 [L3d + Na]⁺, 396 [L3d + K]⁺, 715 [2L3d + H]⁺, 737 [2L3d + Na]⁺, 753 [2L3d + K]⁺, 911 [Au(L3d)₂]⁺.

[Au^{III}Cl(L1e)] (5). Yield: 43% (25 mg). Anal. Calcd for C₁₅H₂₁AuClN₅S₂: C, 31.72; H, 3.73; N, 12.33; S, 11.29%. Found: C, 30.97; H, 3.16; N, 12.03; S, 11.45%. IR (ν_{max} /cm⁻¹): 1558 m (C=N), 1503 vs (C=C), 343 w (Au-Cl). ¹H NMR (CDCl₃, ppm): 1.14 (t, *J* = 7.1 Hz, 3H, CH₃), 1.23 (t, *J* = 7.1 Hz, 3H, CH₃), 2.83 (s, 6H, N-CH₃), 3.64 (q, *J* = 7.1 Hz, 4H, methylene), 7.26–7.29 (m, 3H, Ph), 7.55 (d, *J* = 6.7 Hz, 2H, *o*-Ph). ¹³C NMR (CDCl₃, δ , ppm): 12.8, 13.0 (CH₃), 41.9 (N-CH₃), 45.2, 47.4 (N-CH₂), 127.2, 129.0, 129.4, and 138.0 (Ph), 154.1 (C=N), 157.5 (C=N), 161.4 (C=N). ESI⁺ MS (*m/z*, assignment): 532 [M-Cl]⁺, 568 [M+H]⁺, 590 [M + Na]⁺, 606 [M+K]⁺, 867 [Au(L1e)(L2e)]⁺.

[Au^{III}Cl(L1f)] (6). Yield: 61% (38 mg). Anal. Calcd for C₁₉H₂₉AuClN₅S₂: C, 36.57; H, 4.68; N, 11.22; S, 10.28%. Found: C, 36.19; H, 3.62; N, 10.81; S, 10.57%. IR (ν_{max} /cm⁻¹): 1552 m (C=N), 1497 vs (C=C), 347 w (Au-Cl). ¹H NMR (CDCl₃, ppm): ¹H NMR (CDCl₃, ppm): 0.64 (t, *J* = 7.7 Hz, 6H, -CH₂CH₂CH₃), 1.13 (t, *J* = 7.0 Hz, 3H, -CH₂CH₃), 1.23 (t, *J* = 7.0 Hz, 3H, -CH₂CH₃), 1.38 (sex, *J* = 7.7, 4H, -CH₂CH₂CH₃), 3.03 (t, *J* = 7.7 Hz, 4H, -CH₂CH₂CH₃), 3.62 (m, 4H, -CH₂CH₃), 7.25–7.27 (m, 3H, Ph), 7.45 (d, *J* = 6.6 Hz, 2H, *o*-Ph). ¹³C NMR (CDCl₃, δ , ppm): 11.0, 12.8, 12.9 (CH₃), 21.3 (CH₂, *n*-propyl), 45.1, 47.4 (NCH₂, ethyl), 54.8 (NCH₂, *n*-propyl), 127.3, 128.5, 128.8, 138.4 (Ph), 153.8, 157.3, 159.9 (C=N). ESI⁺ MS (*m/z*, assignment): 588 [M-Cl]⁺, 624 [M+H]⁺, 646

[M + Na]⁺, 662 [M+K]⁺, 979 [Au(L1f)(L2f)]⁺, 1269 [2M+Na]⁺, 1285 [2M+K]⁺. Molar conductivity (10⁻³ M, DMSO): 2.9 S cm² mol⁻¹. High resolution MS of molecular ion [M+H]⁺ Calcd: 624.1297, Found: 624.1277.

Synthesis of the [Au^{III}(SCN)(L1)] Type Complexes. To a solution containing the corresponding [AuCl(L1)] complex (0.05 mmol) in CH₂Cl₂ (1 mL), NH₄(SCN) (0.1 mmol) was added dissolved in MeOH (1 mL). The resulting solution was stirred for 1 h at room temperature and left for slow evaporation of the solvent for 2 days. The green-brown crystalline precipitates formed were filtered off, washed with cold MeOH, and dried under vacuum. Crystals suitable for X-ray diffraction studies were obtained for [Au(SCN)(L1c)].

[Au^{III}(SCN)(L1a)] (7). Yield: 83% (27 mg). Anal. Calcd for C₂₁H₂₃AuN₆S₃: C, 38.65; H, 3.55; N, 12.88; S, 14.74%. Found: C, 38.28; H, 2.98; N, 12.73; S, 14.90%. IR (ν_{max} /cm⁻¹): 2131 w (CN, thiocyanate), 1555 m (C=N), 1497 vs (C=C). ¹H NMR (CDCl₃, ppm): 1.18 (t, *J* = 7.1 Hz, 3H, CH₃), 1.26 (t, *J* = 7.1 Hz, 3H, CH₃), 3.14 (s, 3H, N-CH₃), 3.69 (m, 4H, methylene), 7.16–7.32 (m, 8H, Ph), 7.61–7.63 (m, 2H, *o*-Ph). ¹³C NMR (CDCl₃, δ , ppm): 12.9, 13.0 (CH₃), 43.8 (NCH₃), 45.5, 47.5 (NCH₂), 111.8 (SCN), 126.8, 127.2, 127.4, 129.2, 129.4, 129.6, 137.4, 146.0 (Ph), 155.6 (C=N), 157.1 (C=N), 159.5 (C=N). ESI⁺ MS (*m/z*, assignment): 653 [M+H]⁺, 675 [M + Na]⁺, 691 [M+K]⁺, 991 [Au(L1a)(L2a)]⁺, 1343 [2 M + K]⁺, 1979 [3 M + Na]⁺. Molar conductivity (10⁻³ M, DMSO): 2.6 S cm² mol⁻¹. High resolution MS of molecular ion [M+K]⁺ Calcd: 691.0449, Found: 691.0315.

[Au^{III}(SCN)(L1c)] (8). Yield: 88% (28 mg). Found: C, 34.14; H, 3.75; N, 13.12; S, 15.62. Anal. Calcd for C₁₈H₂₃AuN₆OS₃: C, 34.18; H, 3.66; N, 13.29; S, 15.20. IR (ν_{max} /cm⁻¹): 2129 m (CN, S-bonded thiocyanate), 1558 m (C=N), 1508 vs (C=C). ¹H NMR (CDCl₃, ppm): 1.17 (t, *J* = 7.1 Hz, 3H, CH₃), 1.26 (t, *J* = 7.1 Hz, 3H, CH₃), 3.20 (t, *J* = 4.8 Hz, 4H, N-CH₂), 3.56 (t, *J* = 4.8 Hz, 4H, O-CH₂), 3.66–3.70 (m, 4H, methylene), 7.27–7.32 (m, 3H, Ph), 7.54 (d, *J* = 7.9 Hz, 2H, *o*-Ph). ¹³C NMR (CDCl₃, δ , ppm): 12.9, 13.0 (CH₃), 45.6, 47.6 (NCH₂, ethyl), 49.9 (NCH₂, morpholine), 66.5 (OCH₂), 111.7 (SCN), 127.4, 129.5, 129.6, 137.2 (Ph), 155.5 (C=N), 156.8 (C=N), 160.3 (C=N). ESI⁺ MS (*m/z*, assignment): 574 [M-(SCN)]⁺, 633 [M+H]⁺, 655 [M + Na]⁺, 671 [M+K]⁺, 951 [Au(L1c)(L2c)]⁺, 1287 [2 M + K]⁺, 1919 [3 M + Na]⁺. High resolution MS of molecular ion [M+H]⁺ Calcd: 633.0839, Found: 633.0830.

Synthesis of the [Au(CN)(L1)] Type Complexes. To a solution containing the corresponding [AuCl(L1)] type complex (0.05 mmol) in CH₂Cl₂ (1 mL), were added 2 equiv of KCN (0.1 mmol) dissolved in MeOH (2 mL). The resulting solution was stirred for 15 min at room temperature. Slow evaporation of the solvent gave dark red crystalline precipitates. The crystals formed were filtered off, washed with cold MeOH, and dried under vacuum. Crystals suitable for X-ray diffraction studies were obtained for [Au(CN)(L1c)] and [Au(CN)(L1d)].

[Au^{III}(CN)(L1c)] (9). Yield: 53% (16 mg). Anal. Calcd for C₁₈H₂₃AuN₆OS₂: C, 36.00; H, 3.86; N, 13.99; S, 10.68%. Found: C, 35.74; H, 3.06; N, 13.60; S, 10.93. IR ($\nu_{\max}/\text{cm}^{-1}$): 2175 vw (C≡N), 1564 m (C=N), 1504 vs (C=C), 436 w (Au–C). ¹H NMR (CDCl₃, ppm): 1.18 (t, *J* = 7.0 Hz, 3H, CH₃), 1.26 (t, *J* = 7.0 Hz, 3H, CH₃), 3.23 (t, *J* = 4.8 Hz, 4H, N–CH₂), 3.57 (t, *J* = 4.8 Hz, 4H, O–CH₂), 3.70 (m, 4H, methylene), 7.28–7.32 (m, 3H, Ph), 7.53 (d, *J* = 6.0 Hz, 2H, *o*-Ph). ¹³C NMR (CDCl₃, δ , ppm): 12.8, 13.0 (CH₃), 45.7, 47.5 (NCH₂, ethyl), 50.0 (NCH₂, morpholine), 66.5 (OCH₂), 102.3 (C=N), 127.3, 129.6, 129.6, 137.2 (Ph), 155.6 (C=N), 157.4 (C=N), 161.4 (C=N). ESI⁺ MS (*m/z*, assignment): 601 [M+H]⁺, 623 [M + Na]⁺, 639 [M+K]⁺, 1223 [2 M + Na]⁺, 1823 [3 M + Na]⁺.

[Au^{III}(CN)(L1d)] (10). Yield: 49% (15 mg). Anal. Calcd for C₂₀H₂₇AuN₆S₂: C, 39.22; H, 4.44; N, 13.72; S, 10.47%. Found: C, 38.46; H, 2.80; N, 13.27; S, 11.08%. IR ($\nu_{\max}/\text{cm}^{-1}$): 2172, 2133 vw (C≡N), 1556 m (C=N), 1501 vs (C=C), 444 w (Au–C). ¹H NMR (CDCl₃, ppm): 1.16 (t, *J* = 6.7 Hz, 3H, CH₃), 1.24 (t, *J* = 6.7 Hz, 3H, CH₃), 1.4–1.6 (m, 8H, CH₂ azepine), 3.35 (t, *J* = 5.6 Hz, 4H, N–CH₂), 3.67 (t, *J* = 6.8 Hz, 4H, NCH₂CH₃), 7.26–7.29 (m, 3H, Ph), 7.53 (d, *J* = 7.0 Hz, 2H, *o*-Ph). ¹³C NMR (CDCl₃, δ , ppm): 12.9 (CH₃), 26.9, 28.4 (CH₂, azepine), 45.5, 47.3 (NCH₂, ethyl), 52.9 (NCH₂, azepine), 103.1 (C=N), 127.2, 129.1, 129.4, 137.2 (Ph), 154.8, 156.1, 160.4 (C=N). ESI⁺ MS (*m/z*, assignment): 613 [M+H]⁺, 635 [M + Na]⁺, 651 [M+K]⁺.

X-ray Crystallography. The intensities for the X-ray determinations were collected on a STOE IPDS 2T instrument with Mo K α radiation (λ = 0.71073 Å). Standard procedures were applied for data reduction and absorption correction. Structure solution and refinement were performed with SHELXS-97 and SHELXL-97.¹⁵ Hydrogen atom positions were calculated for idealized positions and treated with the "riding model" option of SHELXL. More details on data collections and structure calculations are contained in Table 1.

Biochemicals and Biological Studies. *Cell Culture Conditions.* The human MCF-7 breastcancer cell line was obtained from the American type Culture Collection (ATCC). This cell line was maintained as a monolayer culture in L-glutamine containing Dulbeccos Modified Eagles Medium (DMEM) with 4.5 g/L glucose (PAA Laboratories GmbH, Austria), supplement with 10% fetal calf serum (FCS; Gibco, Germany) using 25 cm² culture flasks in a humidified atmosphere (5% CO₂) at 37 °C. The cell lines were passaged twice a week after previous treatment with trypsin (0.05%) / ethylenediaminetetraacetic acid (0.02% EDTA; Boehringer, Germany). Jurkat cells were purchased from the German Collection of Microorganisms and Cell Culture (Deutsche Sammlung von Mikroorganismen und Zellkulturen, Braunschweig), DSMZ No ACC 282, LOT 7. The cells were maintained in RPMI 1640 (PAA) medium supplemented with 10% fetal calf serum (PAA), 37 °C, 5% CO₂, and maximum humidity.

In Vitro Chemosensitivity Assay. The in vitro testing of the substances for antitumor activity in adherent growing cell lines was carried out on exponentially dividing human cancer cells according to a previously published microtiter assay.¹⁶ Exponential cell growth was ensured during the whole time of incubation. Briefly, 100 μ L of a cell suspension was placed in each well of a 96-well microtiter plate at 7200 cells/mL of culture medium and incubated at 37 °C in a humidified atmosphere (5% CO₂) for 3 d. By removing the old medium and adding 200 μ L of fresh medium containing an adequate volume of a stock solution of metal complex, the desired test concentration was obtained. Cisplatin was dissolved in dimethylformamide (DMF) while dimethylsulfoxide (DMSO) was used for all other compounds. Eight wells were used for each test concentration and for the control, which

contained the corresponding amount of DMF and DMSO, respectively. The medium was removed after reaching the appropriate incubation time. Subsequently, the cells were fixed with a solution of 1% (v/v) glutaric dialdehyde in phosphate buffered saline (PBS) and stored under PBS at 4 °C. Cell biomass was determined by means of a crystal violet staining technique as described earlier.¹⁷ The effectiveness of the complexes is expressed as corrected T/C_{corr} [%] or τ [%] values according to the following equation:

$$\text{cytostatic effect: } T/C_{\text{corr}}[\%] = [(T - C_0)/(C - C_0)] \times 100$$

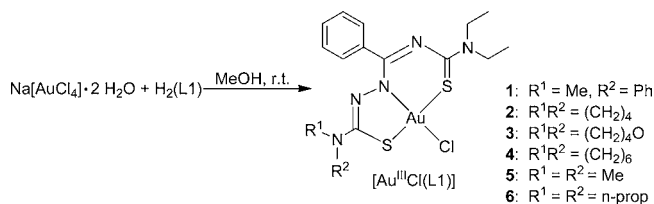
$$\text{cytotoxic effect: } \tau[\%] = [(T - C_0)/C_0] \times 100$$

whereby *T* (test) and *C* (control) are the optical densities at 590 nm of crystal violet extract of the cells in the wells (i.e., the chromatin-bound crystal violet extracted with ethanol (70%) with *C*₀ being the density of the cell extract immediately before treatment. For the automatic estimation of the optical density of the crystal violet extract in the wells, a microplate autoreader (Flashscan S 12; Analytik Jena, Germany) was used.

RESULTS AND DISCUSSION

Reactions of H₂L1 with Na[AuCl₄]·2H₂O in MeOH at room temperature afford analytically pure microcrystalline green precipitates of the composition [AuCl(L1)] in good yields (Chart 2). These products are soluble in CH₂Cl₂, CHCl₃, acetone and DMSO and almost insoluble methanol or ethanol.

Chart 2. Synthesis of the Gold(III) Complexes



The IR spectra of H₂L1 are characterized by strong broad NH absorptions in the range 3140–3240 cm⁻¹ and very strong and sharp bands around 1630 cm⁻¹, which can be assigned to C=N stretches. In the spectra of the gold(III) complexes the NH absorptions are not observed, as expected for the double deprotonation of the ligands during the reaction and the formation of neutral compounds. The C=N stretches are found in the region between 1558 and 1547 cm⁻¹, which corresponds to a bathochromic shift of the $\nu_{\text{C=N}}$ stretches of about 80 cm⁻¹ compared to those of the uncoordinated ligand and indicates chelate formation with a large degree of π -electron delocalization within the chelate rings. Weak absorptions in the range between 335 and 347 cm⁻¹ can be assigned to the ν_{AuCl} stretching bands.

The ¹H NMR spectra of the complexes show the signals in the expected regions.¹⁰ The signals of the two NH protons, which appear as very broad singlets in the region between 10.11 and 9.49 ppm for the free ligands are expectedly not observed in the ¹H NMR spectra of the complexes. This fact confirms the double deprotonation of the ligands which was also confirmed by the IR data.

The ¹³C NMR spectra show the expected signals in the appropriate regions. For the uncoordinated thiosemicarbazides, the C=N and C=S signals of thiourea residues appear in the regions around 149 ppm and 183 ppm, while the C=S resonances of the thiosemicarbazide moiety appear around 179

ppm, as discussed before.¹⁰ Upon coordination and formation of the $[\text{AuCl}(\text{L1})]$ complexes, a downfield shift is observed for the ^{13}C NMR signals of the $\text{C}=\text{N}$ (around 5 ppm), while the $\text{C}=\text{S}$ carbon atom signals are upfield shifted, appearing between 158 and 160 ppm. This is consistent with the $\text{S}_2\text{N}_2\text{S}$ -coordination and thioenolization of the $\text{C}=\text{S}$ of thiourea and thiosemicarbazone moieties.

Figure 1 illustrates the molecular structure of the $[\text{Au}^{\text{III}}\text{Cl}(\text{L1d})]$ (4) as representative of the $[\text{Au}^{\text{III}}\text{Cl}(\text{L1})]$ complexes.

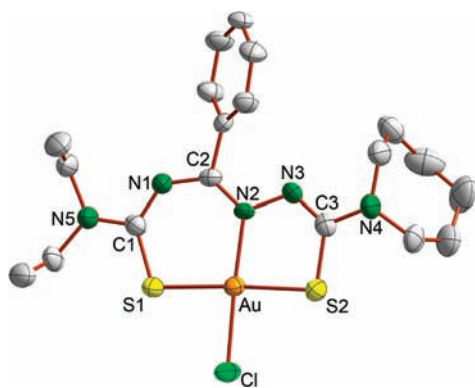


Figure 1. Molecular structure of the complex $[\text{Au}^{\text{III}}\text{Cl}(\text{L1d})]$ (4). Hydrogen atoms omitted for clarity.

Selected bond lengths and angles for this gold(III) complex are shown together with the values of compound 5 in Table 2. The arrangement around the gold atom is best described as slightly distorted square-planar. The thiosemicarbazone binds the gold atom as $\text{S}_2\text{N}_2\text{S}$ -chelate with double-deprotonation of the coordinating backbone. Thus, the square plane is defined by the donor atoms of the tridentate ligand and a remaining chloro ligand, with the maximum deviation from the mean least-squares plane of 0.010 Å for N2. The observed $\text{Au}-\text{Cl}$ and $\text{Au}-\text{S}$ bond lengths are similar to previously reported values for comparable gold(III) thiosemicarbazones.^{6a,7} A considerable delocalization of π -electron density in the six- and five-membered rings is evidenced by the observed bond lengths. The $\text{C}-\text{S}$ and $\text{C}-\text{N}$ bonds inside the chelate rings are within the ranges between carbon-sulfur and carbon-nitrogen single and double bonds, respectively. The $\text{Au}-\text{S1}$ and $\text{Au}-\text{S2}$ bond distances are quite similar; showing strong bond length equalization, which also influences the planarity of the ligand, and makes the bonding backbone almost planar.

The reduction of $\text{Au}(\text{III})$ by thiosemicarbazones is not unexpected and has been reported in several examples before.

In the case of the $\text{H}_2\text{L1}$ ligands, however, this reaction pathway plays a marginal role only, and just in the case of $\text{H}_2\text{L1d}$ a significant amount of the reduction product could be isolated by slow evaporation of the mother solution as colorless crystals (Chart 3). In the IR spectra of these crystals a very strong band in the $\text{C}=\text{N}$ region is observed at 1585 cm^{-1} . In the ^1H NMR spectrum of the compound, the signals are found downfield shifted with respect to those in the spectrum of the gold(III) complex $[\text{Au}^{\text{III}}\text{Cl}(\text{L1d})]$. In contrast to the situation in the ^{13}C NMR spectra of the compounds $\text{H}_2\text{L1}$ and the $[\text{AuCl}(\text{L1})]$ complexes, the rotation around the $\text{C}-\text{NR}_1\text{R}_2$ bonds of the thiosemicarbazide unit is restricted in the gold(I) complex $[\text{Au}^{\text{I}}\text{Cl}(\text{L3d})]$. This is indicated by the appearance of ^{13}C NMR signals for magnetically nonequivalent carbon atoms of the hexamethyleneimine substituent. The observation of a signal at 180.6 ppm is indicative for the coordination of the L3d ligand in its thione form in the gold(I) complex.

The ESI MS spectrum of the colorless gold(I) compound indicated a rearrangement of the organic ligands and the formation of a heterocyclic species after the abstraction of a sulfur atom. Finally, the nature of the side-product could be resolved with an X-ray structural analysis. Figure 2 shows the molecular structure of the product, which represents the expected gold(I) complex with an unusual thiourea ligand together with selected bond lengths and angles. The structure shows that the reduction of the gold atom occurs with a cyclization of the $\{\text{L1d}\}^{2-}$ ligand and sulfur abstraction. The resulting *N*-(hexamethylene)-*N'*-1-(5-diethylamino-3-phenyl-1,2,4-triazolyl)thiourea (L3) acts as a monodentate ligand in the product. A linear coordination environment, which is completed by a chloro ligand, has been found for the gold atom. The triazole ring system is perfectly planar with a maximum deviation of 0.006 Å for the N1 atom. The $\text{C}-\text{S}$ bond of 1.708(5) Å is slightly elongated from a double bond, which is related with the coordination to gold.

Since the $[\text{Au}^{\text{III}}\text{Cl}(\text{L1})]$ compounds are stable both in the solid state and also in solvents like CH_2Cl_2 , CHCl_3 , or DMSO even under reflux conditions for several hours, the formation of the gold(I) complexes occurs most probably parallel to that of the gold(III) complexes. The minor amounts of the side-products, which could be detected for all other $\text{H}_2\text{L1}$ derivatives, except than $\text{H}_2\text{L1d}$, did not allow the isolation of the $\text{Au}(\text{I})$ compounds in pure form.

Nevertheless, there is a strong hint from the mass spectra of all $[\text{AuCl}(\text{L1})]$ complexes, that under high-energy conditions cyclization reactions occur. Besides the expected molecular peaks for the gold(III) complexes $[\text{AuCl}(\text{L1})]$, there appear

Table 2. Selected Bond Lengths (Å) and Angles (deg) in $[\text{Au}^{\text{III}}\text{Cl}(\text{L1d})]$ (4) and $[\text{Au}^{\text{III}}\text{Cl}(\text{L1e})]$ (5)

	4	5		4	5
$\text{Au}-\text{Cl}$	2.308(2)	2.291(2)	$\text{N1}-\text{C2}$	1.352(9)	1.34(1)
$\text{Au}-\text{S1}$	2.282(2)	2.289(2)	$\text{C2}-\text{N2}$	1.295(9)	1.318(9)
$\text{Au}-\text{N2}$	2.018(5)	2.015(6)	$\text{N2}-\text{N3}$	1.394(8)	1.384(9)
$\text{Au}-\text{S2}$	2.287(2)	2.286(2)	$\text{N3}-\text{C3}$	1.286(0)	1.29(1)
$\text{C1}-\text{N1}$	1.317(9)	1.31(1)	$\text{C3}-\text{S2}$	1.768(8)	1.747(8)
$\text{C1}-\text{S1}$	1.734(8)	1.733(9)	$\text{C1}-\text{N5}$	1.349(0)	1.34(1)
$\text{S1}-\text{Au}-\text{S2}$	176.87(7)	176.20(8)	$\text{N2}-\text{Au}-\text{Cl}$	176.80(7)	175.3(2)
$\text{N2}-\text{Au}-\text{S1}$	97.12(7)	99.0(2)	$\text{S1}-\text{Au}-\text{Cl}$	86.03(7)	85.51(8)
$\text{N2}-\text{Au}-\text{S2}$	86.03(7)	84.8(2)	$\text{S2}-\text{Au}-\text{Cl}$	90.85(7)	90.69(8)
$\text{C1}-\text{S1}-\text{Au}$	106.2(3)	105.1(3)	$\text{N3}-\text{N2}-\text{Au}$	117.3(4)	119.4(5)
$\text{C3}-\text{S2}-\text{Au}$	94.2(3)	94.9(3)	$\text{C2}-\text{N2}-\text{Au}$	126.8(5)	124.2(5)

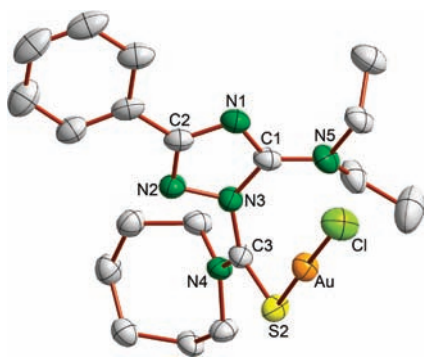
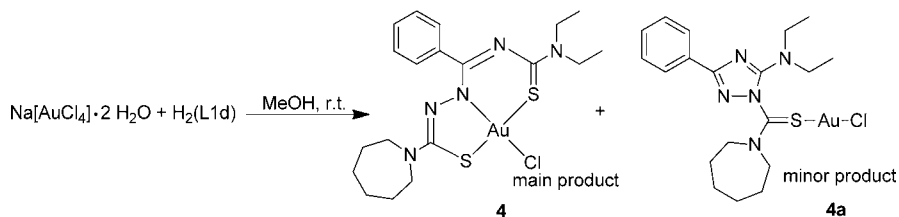
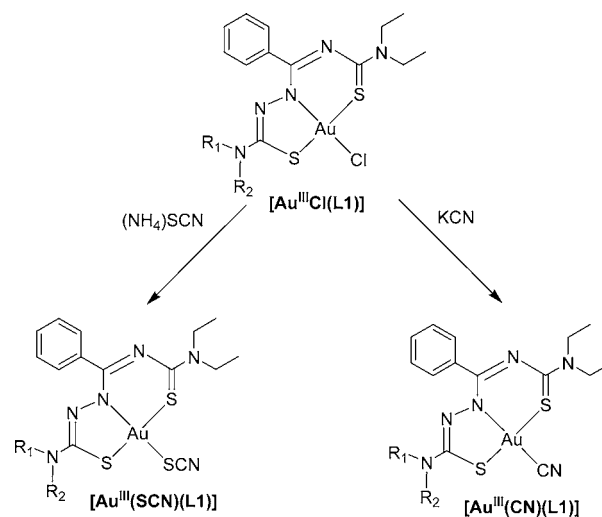
Chart 3. Formation of a Au^I Side-Product during the Reaction with H₂L1d

Figure 2. Structure of the complex $[\text{Au}^{\text{I}}\text{Cl}(\text{L3d})]$ (**4a**). Hydrogen atoms are omitted for clarity. Selected bond length (Å) and angles (deg): Au–Cl 2.271(1), Au–S 2.261(1), S2–C3 1.708(5), C3–N3 1.404(5), Cl–Au–S2 176.80(5), Au–S2–C3 108.9(2).

peaks for species of the composition $[\text{Au}(\text{L1})(\text{L2})]^+$, where L2 corresponds to the primary cyclization product of the corresponding thiosemicarbazone (Chart 4). As the samples were crystalline and analytically pure, these species were formed under measurement conditions. The observation of the coordinated species L2 in the ESI⁺ MS spectra of almost all Au(III) complexes studied and the crystallographic characterization of the final decomposition product L3d in complex **4a** allow the formulation of a pathway for the cyclization of the ligands under the influence of gold ions (Chart 4). It should be mentioned, that the MS spectra of the compounds H₂L1 do not give any evidence for similar reactions.

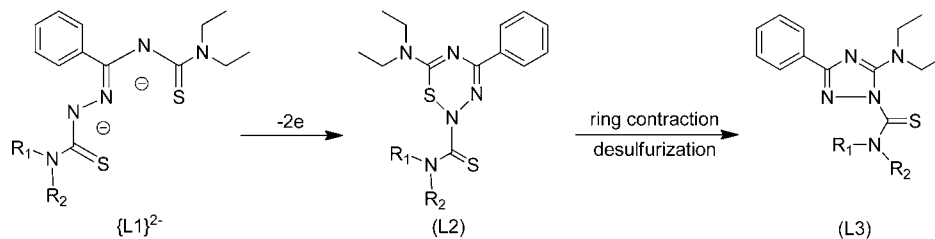
The chloro ligands in the $[\text{Au}^{\text{III}}\text{Cl}(\text{L1})]$ complexes are readily replaced by SCN[−] or CN[−] ligands without any change in the oxidation state of the metal. Such reactions proceed at room temperature in mixtures of CH₂Cl₂ and MeOH, which yield the products as crystalline solids in excellent yields (Chart 5). First evidence of the successful exchange reaction with SCN[−] was the IR spectrum of the resulting solid, which expectedly shows only marginal shift of the band, which belong to the thiosemicarbazone, but an additional band at about 2130 cm^{−1}, which can be assigned to the coordination of S-bonded thiocyanate.^{18,19} ¹H and ¹³C NMR spectra of $[\text{Au}(\text{SCN})(\text{L1})]$ complexes are very similar to those of the analogous chloro

Chart 5. Formation of the $[\text{Au}(\text{X})(\text{L1})]$ Complexes (X = SCN or CN)

complexes. Additional ¹³C NMR signals around 112 ppm can be assigned to the coordinated SCN[−] ligands. The corresponding signal of potassium thiocyanate in water appears at 133.3 ppm.²⁰

Crystals suitable for structural analysis were obtained for the complex $[\text{Au}(\text{SCN})(\text{L1c})]$ (**8**). The crystals appear as orange-brown plates. Figure 3 illustrates the molecular structure of **8** as the representative compound of such complexes together with selected bond lengths and angles. The bonding situation inside the organic ligand is only a little different from those observed for the chloro complexes. All C–S and C–N bonds inside the chelate rings are practically in the same ranges as observed for **4** and **5**, but a stronger bond-length equalization of the C–N bonds is observed, which is also extended to the C1–N5 bond. The thiocyanato ligand shows the typical bent coordination, with an Au–S–C angle of 105.0(3)°, and the arrangement of the SCN[−] ligand is coplanar with the coordination sphere of the thiosemicarbazonato ligand in a way that the thiocyanate ligand lies almost parallel to the Au–S2 bond.

The ongoing discussion about the role of cyano species in the metabolism of gold drugs and the fact that stable CN[−]

Chart 4. Proposed Pathway for the Cyclization of H₂L1 Based on the Ionization of the Complexes

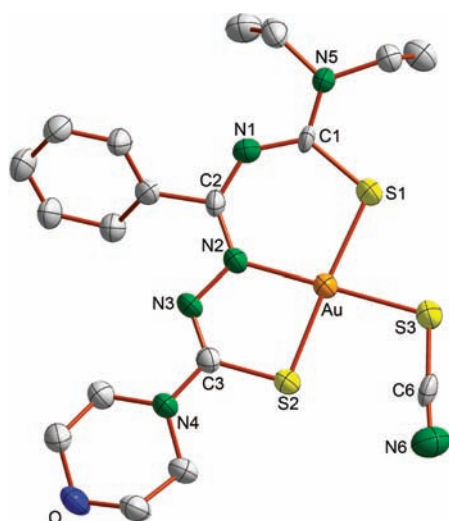


Figure 3. Molecular structure of the complex $[\text{Au}^{\text{III}}(\text{SCN})(\text{L1c})]$ (8). Hydrogen atoms omitted for clarity. Selected bond length (Å) and angles (deg): Au–S1 2.290(3), Au–S2 2.280(2), Au–S3 2.323(3), Au–N2 2.022(8), S1–C1 1.775(9), C1–N1 1.32(1), N1–C2 1.32(1), C2–N2 1.34(1), N2–N3 1.388(9), N3–C3 1.27(1), C3–S2 1.77(1), S3–C6 1.66(1), C6–N6 1.15(1), S1–Au–N2 98.3(2), S1–Au–S2 176.6(1), S1–Au–S3 81.6(3), N2–Au–S2 84.7(2), N2–Au–S3 179.7(3), S2–Au–S3 95.37(9), Au–S3–C6 105.0(3), S3–C6–N6 176.1(1).

compounds are known for Au(I) and Au(III) stimulated us to include CN^- ligands in the present study.^{3b,20} $[\text{Au}(\text{CN})(\text{L1c})]$ and $[\text{Au}(\text{CN})(\text{L1d})]$ are formed during reactions of the corresponding chloro complexes with KCN in MeOH/ CH_2Cl_2 mixtures. The products can be isolated in crystalline forms after slow evaporation of the reaction mixtures. In the IR spectra of these complexes, bands appear in the ranges between 2130 and 2175 cm^{-1} and $436\text{--}444\text{ cm}^{-1}$, which are related to ν_{CN} and ν_{AuC} stretching vibrations, respectively.¹⁸ The relatively high frequencies of the ν_{CN} stretches are indicative of a strong σ -donation in these gold(III) complexes since electrons are removed from the 5σ orbital, which is weakly antibonding, while π -backbonding tends to decrease the ν_{CN} because the electrons enter into the antibonding $2p\pi^*$ orbital.¹⁶ The ^1H NMR spectra of the cyano complexes are similar to those of the $[\text{Au}(\text{SCN})(\text{L1})]$ type complexes and reflect a similar bonding situation. In the ^{13}C NMR spectra of the $[\text{Au}(\text{CN})(\text{L1})]$ complexes, signals are found around 102 ppm, which confirm the presence of cyanide coordinated to gold(III) centers. The chemical shift for free cyanide is at 163.6 ppm and for $[\text{Au}(\text{CN})_4]^-$ a value of 103.5 ppm was found in CD_3OD .²¹ ESI⁺ mass spectra of **9** and **10** exhibit the expected molecular ion peaks and the peaks related to the $[\text{M}+\text{H}]^+$. $[\text{Au}(\text{L1})(\text{L2})]^+$ species are not observed here, which may indicate that the Au–C bond is stronger than the Au–Cl and Au–SCN bonds and hinders the cyclization.

Figure 4 illustrates the molecular structure of **9** as an example of the compounds. Selected bond lengths and angles for the complexes **9** and **10** are compared in Table 3. There are no significant differences in the bonding situation of the thiosemicarbazonato ligands between the chloro and the cyano derivatives.

Many efforts in pharmaceutical gold chemistry have been dedicated to the development of antitumor agents on the basis of both Au(I) and Au(III) compounds.^{3b,22–29} Recent research

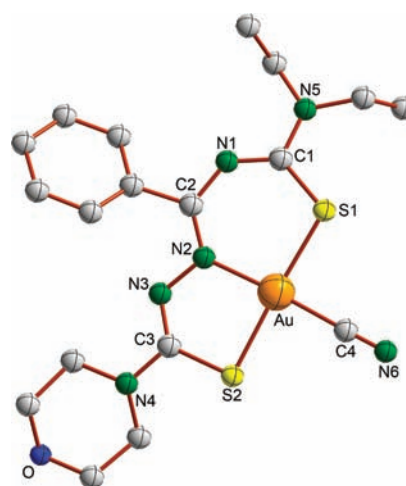


Figure 4. Molecular structure of the complex $[\text{Au}^{\text{III}}(\text{CN})(\text{L1c})]$ (9). Hydrogen atoms omitted for clarity.

has also included gold complexes with N-heterocyclic carbenes,^{30,31} and a number of cationic complexes with a variety of preferably N-donor ligands.^{32–34} The latter compounds show good to moderate cytotoxicities in cancer cell lines including cisplatin-resistant cells.

Thiosemicarbazones exhibit various biological activities and have therefore attracted considerable pharmaceutical interest. Several mechanisms of antitumor action were proposed and compelled the interest of an SAR study. Furthermore, it is well-known that such compounds are potent metal chelators and the cytotoxic properties of the compounds are influenced by chelation. In many cases, an increased activity of the metal complexes is observed, which is assumed to be an effect of a metal-assisted transport, while complex dissociation inside the cell releases the thiosemicarbazones as the biologically active species.³⁵ The compounds presented here represent a new series of familiar compounds, which combine ligands with potential biological activity with metal ions with pharmaceutical potential. To obtain an overview of the influence of the individual residues in the molecular framework of the thiosemicarbazones, we modified R^1 and R^2 (compounds $\text{H}_2\text{L1a}$ to $\text{H}_2\text{L1e}$) and prepared the corresponding gold(III) complexes $[\text{AuCl}(\text{L1})]$. The exchange of the chloro ligands by SCN^- and CN^- may allow an insight into the mechanism of potential activity and the role of the relatively labile Cl^- ligand.

Thus, we investigated the antiproliferative effects of the ligands in relation to their $[\text{AuCl}(\text{L1})]$ complexes in a time response as well as in a concentration response assay. From the first study the response of the cells to the compounds can be estimated, while the latter allows the calculation of IC_{50} values. Additionally, each two representatives of the SCN^- and CN^- compounds have been included into this study, to obtain information about the influence of the halide/pseudohalide ligand.

The thiosemicarbazones $\text{H}_2\text{L1}$ cause a strong reduction of the growth of human MCF-7 breast cancer cells. Maximum activity was already detected after an incubation time of 48 h (Figure 5). At the concentrations from 1.25 to $10\ \mu\text{M}$ cytotoxic effects were observed. The rising recuperation of the cells at lower concentrations is characteristic for a cytostatic effect. The time response curve of cisplatin is quite different, with a maximum cytotoxicity appearing not before an incubation time of more than 100 h. All compounds $\text{H}_2\text{L1}$ show this interesting

Table 3. Selected Bond Lengths (Å) and Angles (deg) in [Au(CN)(L1c)] (9) and [Au(CN)(L1d)] (10)

	9	10		9	10
Au–N2	2.015(6)	2.017(6)	C1–S1	1.739(8)	1.731(8)
Au–S1	2.298(2)	2.290(2)	S2–C3	1.775(8)	1.781(8)
Au–S2	2.286(2)	2.287(2)	N3–C3	1.28(1)	1.27(1)
Au–C4	2.003(8)	2.00(1)	N3–N2	1.415(8)	1.410(9)
C2–N1	1.352(9)	1.33(1)	N2–C2	1.302(9)	1.31(1)
C1–N1	1.315(9)	1.34(1)	N5–C1	1.35(1)	1.33(1)
C4–N6	1.12(1)	1.08(2)			
N2–Au–S2	85.9(2)	85.9(2)	N2–Au–S1	97.2(2)	97.3(2)
S2–Au–S1	176.84(8)	176.82(7)	N2–Au–C4	176.8(3)	176.2(3)
S2–Au–C4	90.9(3)	90.7(3)			

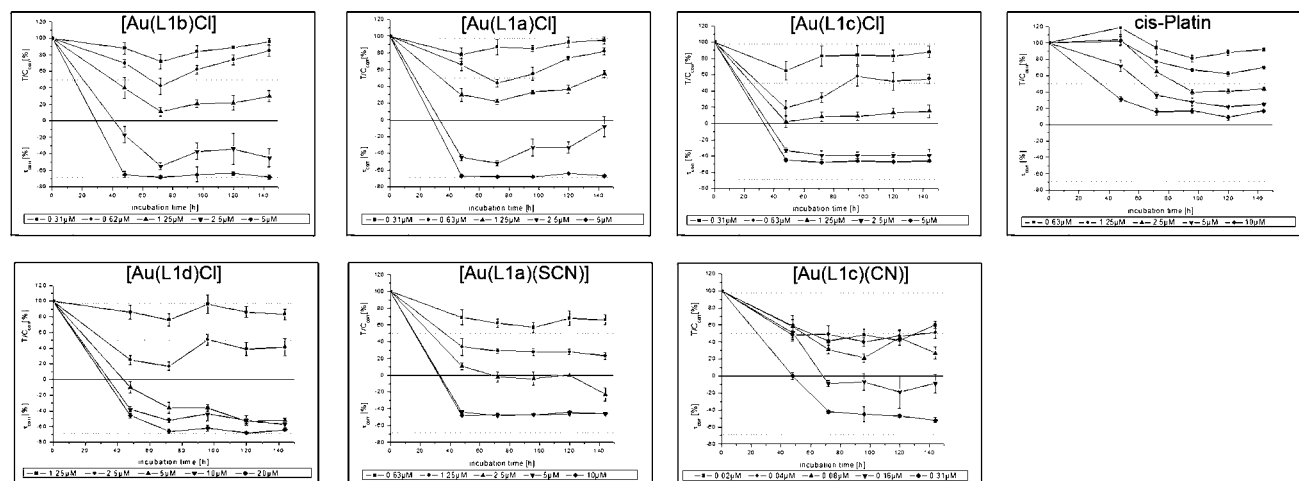


Figure 5. Cytotoxic effects of selected ligands and complexes.

Table 4. Cytotoxic Effects of Ligands H₂L1 and their Gold Complexes against MCF-7 Cells

	R ¹	R ²	Ligand	IC ₅₀ [μM]		
				[Au ^{III} Cl(L1)]	[Au ^{III} (SCN)(L1)]	[Au ^{III} (CN)(L1)]
H ₂ L1a	CH ₃	Phenyl	0.85 ^a	0.68	0.99	
H ₂ L1b		(CH ₂) ₄	2.19 ^a	0.61		
H ₂ L1c		morpholinyl	0.74	0.63	0.35	0.025
H ₂ L1d		(CH ₂) ₆	2.43 ^a	0.66		0.045
H ₂ L1e	CH ₃	CH ₃	0.23 ^a	0.66		
H ₂ L1f	<i>n</i> -propyl	<i>n</i> -propyl	9.04	0.85		

^aValues taken from ref 10.

behavior and comparable time response curves, which allows the comparison of IC₅₀ values (after an incubation time of 48 h, see Table 4). The degree of cytotoxicity can be influenced by the variation of the peripheral substituents R¹ and R² as has already been stated in ref 10.

After coordination of the thiosemicarbazones to Au(III), for most of the compounds a clear increase of the activity can be stated, displaying IC₅₀ values around 0.6 μM, while only for the most active compound H₂L1e is a slight decrease observed upon complex formation. It is obvious that the formation of the gold complexes levels their cytotoxic effects to low concentrations irrespective to their substituents R¹ and R², which clearly implies different mechanisms of the activity for the ligands and their [AuCl(L1)] complexes. With the observed IC₅₀ values, the complexes under study seem to be more active by at least 1 order of magnitude than the previously reported cationic complexes with nitrogen donor atoms.^{33,34} However, it must be mentioned that the mode of action of the present

compounds is hitherto unclear and the thiosemicarbazide ligands themselves possess a considerable degree of activity.

On the other hand the reduction of gold(III) to gold(I) with oxidative cyclization of the thiosemicarbazone, as in the case of the complex [Au^ICl(L3d)], leads to the formation of a much less active compound (IC₅₀: 5.6 μM). After substitution of the chloro ligands by thiocyanato or cyano ones, no considerable changes in the cytotoxicity with respect to the chloro compounds was observed for the SCN⁻ complexes, while the activity is significantly increased for the cyano complexes. Hence, this may imply that the [AuCl(L1)] and [Au(SCN)(L1)] complexes have the same target in the cell. The effect that can be obtained with the CN⁻ substitution will be subject of further studies, also including other cyano complexes of gold. In many cases, also with thiosemicarbazone ligands, a metal-assisted transport is discussed as the reason for higher activities of metal complexes when compared with their uncoordinated organic ligands, while complex dissociation inside the cell

releases the thiosemicarbazones as the biologically active species. Our results, however, show that a simple complex dissociation mechanism is less probable for the compounds under study in this work, since the time response curves for the gold(III) complexes differ substantially from those of the uncoordinated thiosemicarbazones, and oxorhenium(V) complexes of the type $[\text{ReOCl}(\text{L}1)]$, which have been studied in a previous work.¹⁰

Presently, studies with further systematic variations of the molecular framework are underway in our laboratories. They also include the quest for the point of attack of the active compounds and the role of the metal ion (and the coligands CN^- or SCN^-) and the intracellular targets. For instance, thiosemicarbazones can stabilize cleavable complexes formed by topoisomerase II (topoII) and DNA leading to apoptosis or they can inhibit ribonucleotide reductase (RR) activity.³⁶ Studies with the radioactive gold isotope ^{198}Au will help to answer the remaining questions and allow further optimization of the promising cancerostatic properties of the new class of complexes.

■ ASSOCIATED CONTENT

📄 Supporting Information

Crystallographic data in CIF format. This material is available free of charge via the Internet at <http://pubs.acs.org>.

■ AUTHOR INFORMATION

Corresponding Author

*E-mail: ulrich.abram@fu-berlin.de.

■ ACKNOWLEDGMENTS

We gratefully acknowledge financial support of DAAD, CAPES, CNPq, and FAPESP.

■ DEDICATION

^{||}Dedicated to Professor Reinhard Kirmse on the occasion of his 65th birthday.

■ REFERENCES

- (1) (a) Christlieb, M.; Dilworth, J. *Chem.—Eur. J.* **2006**, *12*, 6194. (b) West, D. X.; Padhyé, S. B.; Sonawane, P. B. *Structure and Bonding, Complex Chemistry*; Springer: Berlin, Germany, 1991; (c) Casas, J. S.; Garcia-Tasende, M. S.; Sordo, J. *Coord. Chem. Rev.* **2000**, *209*, 197. (d) Yu Yu.; Kalinowski, D. S.; Kovacevic, Z.; Siafakas, A. R.; Jansson, P. J.; Stefani, C.; Lovejoy, D. P.; Sharpe, P. C.; Bernhardt, P. V.; Richardson, D. R. *J. Med. Chem.* **2009**, *52*, 5271. (e) Beraldo, H.; Gambino, D. *Mini-Rev. Med. Chem.* **2004**, *4*, 31.
- (2) (a) Klayman, D. L.; Scovill, J. P.; Bartosevich, J. F.; Mason, C. J. *J. Med. Chem.* **1979**, *22*, 1367. (b) Maia, P. I. S.; Pavan, F. R.; Leite, C. Q. F.; Lemos, S. S.; de Sousa, G. F.; Batista, A. A.; Nascimento, O. R.; Ellena, J.; Castellano, E. E.; Niquet, E.; Deflon, V. M. *Polyhedron* **2009**, *28*, 398.
- (3) (a) Eisler, R. *Inflammation Res.* **2003**, *52*, 487. (b) Tiekink, E. R. T. *Gold Bull.* **2003**, *36*, 117. (c) Ho, S. Y.; Tiekink, E. R. T. Gold-based Therapeutics – Use and Potential. In *Metallotherapeutic Drugs and Metal-Based Diagnostic Agents: The Use of Metals in Medicine*; Gielen, M., Tiekink, E. R. T., Eds.; Wiley: Hoboken, NJ, 2005.
- (4) (a) Kovala-Demertzi, G.; Nath Yadav, P.; Wiecek, J.; Skoulika, S.; Varadinova, T.; Demertzis, M. A. *J. Inorg. Biochem.* **2006**, *100*, 1558. (b) Lobana, T. S.; Khanna, S.; Butcher, R. J. *Inorg. Chem. Commun.* **2008**, *11*, 1433–1435. (c) Castiñeiras, A.; Pedrido, R.; Pérez-Alonso, G. *Eur. J. Inorg. Chem.* **2008**, 5106. (d) Khanye, S. D.; Bathori, N. B.; Smith, G. S.; Chibale, K. *Dalton Trans.* **2010**, *39*, 2697. Khanye, S. D.; Smith, G. S.; Lategan, C.; Smith, P. J.; Gut, J.; Rosenthal, P. J.; Chibale, K. *J. Inorg. Biochem.* **2010**, *104*, 1079.

- (5) Ortner, K.; Abram, U. *Inorg. Chem. Commun.* **1998**, *1*, 251–253.
- (6) (a) Abram, U.; Ortner, K.; Gust, R.; Sommer, K. *J. Chem. Soc., Dalton Trans.* **2000**, 735–744. (b) Casas, J. S.; Castano, M. V.; Cifuentes, M. C.; García-Monteaudo, J. C.; Sánchez, A.; Sordo, J.; Abram, U. *J. Inorg. Biochem.* **2004**, *98*, 1009–1016. (c) Castiñeiras, A.; Dehnen, S.; Fuchs, A.; García-Santos, I.; Sevillano, P. *Dalton Trans.* **2009**, 2731–2739.
- (7) Garcia-Santos, I.; Hagenbach, A.; Abram, U. *J. Chem. Soc., Dalton Trans.* **2004**, 677–682.
- (8) Sreekanth, A.; Fun, H. -K.; Kurup, M. R. P. *Inorg. Chem. Commun.* **2004**, *7*, 1250–1253.
- (9) Bottenus, B. N.; Kana, P.; Jenkins, T.; Ballard, B.; Rold, T. L.; Barnesa, C.; Cutler, C.; Hoffman, T. J.; Green, M. A.; Jurisson, S. A. *Nucl. Med. Biol.* **2010**, *37*, 41.
- (10) Nguyen, H. H.; Jegathesh, J. J.; Maia, P. I. S.; Deflon, V. M.; Gust, R.; Bergemann, S.; Abram, U. *Inorg. Chem.* **2009**, *48*, 9356.
- (11) Sasane, A.; Matuo, T.; Nakamura, D.; Kubo, M. *J. Magn. Reson.* **1971**, *4*, 257.
- (12) Beyer, L.; Widera, R. *Tetrahedron Lett.* **1982**, *23*, 1881.
- (13) Scovill, J. P. *Phosphorus, Sulfur, Silicon Relat. Elem.* **1991**, *60*, 15.
- (14) Nguyen, H. H.; Maia, P. I. S.; Deflon, V. M.; Abram, U. *Inorg. Chem.* **2009**, *48*, 25.
- (15) Sheldrick, G. M. *SHELXS-97 and SHELXL-97, programs for the solution and refinement of crystal structures*; University of Göttingen: Göttingen, Germany, 1997.
- (16) (a) Bernhart, G.; Reile, H.; Birnböck, H.; Spruss, T.; Schönenberger, H. *Cancer Res. Clin. Oncol.* **1992**, *118*, 35. (b) Reile, H.; Birnböck, H.; Bernhardt, G.; Spruss, T.; Schönenberger, H. *Anal. Biochem.* **1990**, *187*, 262.
- (17) Marmur, J. *J. Mol. Biol.* **1961**, *3*, 208.
- (18) Nakamoto, K. *Infrared and Raman Spectra of Inorganic and Coordination Compounds Part B*; John Wiley & Sons: Hoboken, NJ, 2009.
- (19) Fan, D.; Yang, C.-T.; Ranford, J. D.; Vittal, J. J.; Lee, P. F. *Dalton Trans.* **2003**, 3376.
- (20) (a) Pretsch, E.; Clerc, T.; Seibl, J.; Simon, W. *Tables of Spectral Data for Structure Determination of Organic Compounds*, 2nd ed.; Springer: Berlin, Germany, 1989; (b) Levy, G. C.; Lichter, R. L.; Nelson, G. L. *Carbon-13 Nuclear Magnetic Resonance for Organic Chemists*, 2nd ed.; Wiley: New York, 1980.
- (21) Al-Maythaly, B. A.; Wazeer, M. I. M.; Isab, A. A. *J. Coord. Chem.* **2010**, *63*, 3824.
- (22) Nobili, S.; Mini, E.; Landini, I.; Gabbiani, C.; Casini, A.; Messori, L. *Med. Res. Rev.* **2010**, *30*, 550.
- (23) Wang, X. Y.; Guo, Z. *J. Dalton Trans.* **2008**, 1521.
- (24) Ott, I. *Coord. Chem. Rev.* **2009**, *253*, 1670.
- (25) Ronconi, L.; Marzano, C.; Zanello, P.; Corsini, M.; Miolo, G.; Macca, C.; Trevisan, A.; Fregona, D. *J. Med. Chem.* **2006**, *49*, 1648.
- (26) Che, C. M.; Sun, R. W. Y.; Yu, W. Y.; Ko, C. B.; Zhu, N. Y.; Sun, H. Z. *Chem. Commun.* **2003**, 1718.
- (27) Sun, R. W. Y.; Che, C. M. *Coord. Chem. Rev.* **2009**, *253*, 1682.
- (28) Casini, A.; Cinellu, M. A.; Minghetti, G.; Gabbiani, C.; Coronello, M.; Mini, E.; Messori, L. *J. Med. Chem.* **2006**, *49*, 5526.
- (29) Liu, W.; Bendorf, K.; Proetto, M.; Abram, U.; Hagenbach, A.; Gust, R. *J. Med. Chem.* **2011**, 548605.
- (30) Liu, W.; Bendorf, K.; Proetto, M.; Abram, U.; Hagenbach, A.; Gust, R. *J. Med. Chem.*, submitted for publication.
- (31) Mendes, F.; Groessl, M.; Nazarov, A. A.; Tsybin, Y. O.; Sava, G.; Santos, I.; Dyson, P.; Casini, A. *J. Med. Chem.* **2011**, *54*, 2196, and refcited therein.
- (32) Casini, A.; Hartinger, C. G.; Nazarov, A. A.; Dyson, P. *J. Med. Organometallic Chem.* **2011**, *57*, and refs cited therein..
- (33) Casini, A.; Hartinger, C.; Gabbiani, C.; Mini, E.; Dyson, P. J.; Keppler, B. K.; Messori, L. *J. Inorg. Biochem.* **2008**, *102*, 564.
- (34) Casini, A.; Diawara, M. C.; Scopelliti, R.; Zakeeruddin, S. M.; Grätzel, M.; Dyson, P. *J. Dalton Trans.* **2010**, *39*, 2239.
- (35) Scovill, J. P.; Klayman, D. L.; Lambrose, C.; Childs, G. E.; Notsch, J. D. *J. Med. Chem.* **1984**, *27*, 87.

(36) Chen, J.; Huang, Y.-W.; Liu, G.; Afrasiabi, Z.; Sinn, E.; Padhye, S.; Ma, Y. *Toxicol. Appl. Pharmacol.* **2004**, *197*, 40.